

Fabrication of Cerium Oxide Nanoparticles with Improved Antibacterial Potential and Antioxidant Activity

Karthikeyan Kandhasamy and Kumpati Premkumar*

Cancer Genetics and Nanomedicine laboratory, Department of Biomedical Science,
Bharathidasan University, Tiruchirappalli – 620 024, Tamil Nadu, India.

<http://dx.doi.org/10.13005/bbra/3104>

(Received: 03 February 2023; accepted: 08 April 2023)

Recent years have seen a dramatic uptick in both research into and practical application of nanoparticles (NPs). Many biomedical applications have found success with the use of nanoparticles due to their wide spectrum of significant biological effects, including antibacterial and antioxidant properties. Nanoparticles that aren't harmful are gaining traction as a promising new class of antioxidants. Cerium oxide is a lanthanide rare-earth element. Cerium oxide nanoparticles (CNPs) exhibit a large surface area and good catalytic activity, the result of the dual oxidation state of CNPs, Ce^{3+} and Ce^{4+} , has good antibacterial and antioxidant activity. CNPs were characterised by using analytical techniques such as the UV-Visible spectrophotometer, scanning electron microscopy, X-ray diffraction, zeta potential, Fourier transform infrared spectroscopy, and dynamic light scattering (DLS). CNPs exhibited a strong zone of inhibition against *S. aureus* (15mm) and *E. coli* (14mm). In vitro antioxidant activity of CNPs was investigated using the DPPH and ABTS techniques, with 50% of their radical scavenging potential being observed at concentrations of $47.61\mu g/mL$ and $49.26\mu g/mL$ respectively. Thus, our study reports that CNPs could be used as a prominent and efficient antioxidant and antibacterial agent. However, further studies are needed to understand the possible mechanisms of toxicity assessment.

Keywords: Antioxidant; ABTS; Cerium oxide nanoparticles (CNPs); cell wall damage; DPPH.

Nanotechnology is one of the most exciting research frontiers in current materials science because of their unique physiochemical properties¹. Synthesis of metallic nanoparticles with a size range of 1nm to 100 nm or less has a peculiar property, for example, size, shape, and high distribution, with enhanced applications such as the biomedical field². In cancer therapy, nanoparticles worked with minimal side effects and improved pharmacokinetics³.

The metal oxide nanoparticles are used in highly potential biological applications

due to their controlled size, shapes, chemical constituents, and valence state. Among the metal oxide nanoparticles, TiO_2 , FeO_2 and CeO_2 are extremely reactive oxides that acutely interconnect with the metabolic networks of cells⁴. Cerium oxide (CeO_2) is a rare earth metal in the lanthanide family. Among the researchers, cerium oxide nanoparticles are becoming the most significant material due to their two oxidation states, Ce^{3+} and Ce^{4+} as well as their greater oxygen mobility and loading capacity^{5,6}. The cubic fluorite structure of cerium oxide nanoparticles (CNPs) is active

*Corresponding author E-mail: prems@bdu.ac.in



in biomedical applications such as anticancer, antioxidant, antibacterial, bone implant material, device fabrication, and drug carrier^{6,7} due to their topography, size, and biocompatibility⁸. Cerium oxide nanoparticles are active and play a significant role in toxicity against yeast, bacteria, and fungi⁹ by interacting with the microbe's cell wall through electrostatics^{10,11}. The paired oxidation states Ce³⁺ and Ce⁴⁺ of cerium oxide nanoparticles are responsible for the enhanced antibacterial potential. Sufficient dispersibility makes them exist as a catalytic location for the attachment and long-chain phospholipid hydrolysis found on the surface of the bacterial membranes¹². The Ce atom's ability to transition between the 3⁺ and 4⁺ states of oxidation consists of cerium oxide nanoparticles that exhibit autocatalytic activity, which results in a strong radical-scavenging potential whenever this state occurs in a biological system at pH 7.4^{13,14}.

In this present study, we demonstrate CNPs as good hybrid nanomaterials for bacterial growth inhibition *Staphylococcus aureus* and *Escherichia coli* also have good antioxidant potential for radical scavenging that was investigated by using the DPPH and ABTS assays. Further cerium oxide nanoparticles have been characterised using different techniques such as the UV-Visible spectrophotometer, morphology identification using SEM, functional groups of nanoparticles identification by FT-IR, DLS to determine hydrodynamic diameter, Zeta potential analyses to identify the surface charge of nanoparticles, and XRD for confirmation of the crystalline nature of nanoparticles.

MATERIALS AND METHODS

Cerium oxide nanoparticle Synthesis

Cerium oxide nanoparticles were synthesised according to the work of Pinna *et al.*, 2020¹⁴ with some modifications. In 10 mL of 2-propanol, 3.5g of Ce(NO₃)₃·6H₂O was dissolved, and then 1M of 0.25mL HCl was added and stirred until complete dissolution. In a separate vial, 1g of urea was dissolved in 10 mL of 2-propanol that contained 1M of 0.25mL HCl and stirred for 5 minutes. The solution of urea was added dropwise to the Ce(NO₃)₃ solution under stirring conditions, and NH₄OH 7mL was added to that mixture when the addition was complete.

The samples were then microwaved four times at 600 W for 10 seconds before being washed with water and centrifuged at 10,000 rpm. After that, the discarded supernatant (5 mL of suspension) was allocated with a light yellow milky pellet (500mg of CeO₂).

Characterization

UV-visible spectroscopy measurements were performed at room temperature using a spectrophotometer UV-2450 (Shimadzu) and observed in the 200–800 nm range for cerium oxide nanoparticles (CNP). The topographical architecture of CNPs was studied using scanning electron microscopy (SEM) (JSM-6480 LV). The hydrodynamic size of CNPs is measured by DLS, and the surface charge of CNPs is determined by the zeta potential of (ζ) using a Zetasizer Nano ZS (Malvern Instruments Ltd., Malvern, UK). Fourier transform infrared spectroscopy (FT-IR) analysis was performed at a range of 4000–400cm⁻¹ (Perkin Elmer, USA). X-ray diffractometer (XRD) analysis confirmed the crystalline morphology of the CNPs (SmartLab, Rigaku Corporation, Japan).

Investigation of antibacterial activity

Diffusion method in agar well

The antibacterial potential of CNPs was assessed using the agar well diffusion technique against *S. aureus* and *E. coli*. Bacterial culture was spread using cotton swabs on nutrient agar (HiMedia, India) plates. Wells were performed using gel puncture (the diameter of the wells was 6 mm) on nutrient agar plates. In each well added with different doses of CNPs (25-100i_g/mL), streptomycin (HiMedia, India) was used as a positive control (10i_g/mL) and 30iL of autoclaved, double distilled water acted as a negative control. After that, the nutrient agar plates were incubated for 24 hours at 37°C. After the incubation period, the zone of inhibition diameter was measured in mm¹⁵.

Analysis of bacterial Growth curve

Staphylococcus aureus and *Escherichia coli* were treated with different concentrations of CNPs 25, 50, 75, 100i_g/mL which were compared with the untreated bacteria as a control to assess the bacterial growth curve. Briefly, a 96-well microliter plate was filled with 250 iL of LB and 20iL of bacterial suspension (10⁷ CFU/mL) and incubated at 37 °C for 24 hours. Every 3 hours for 24 hours, bacterial growth rate was measured at

580 nm using a Synergy HT Multimode Reader (Biotek, Winooski, USA). The experiments were performed in triplicates¹⁶.

Evaluation of antioxidant activity in *in vitro*

Radical scavenging activity by DPPH method

The scavenging activity of CNPs against 2,2-diphenyl-1-picrylhydrazide (DPPH) (HiMedia, India) was calculated according to the¹⁷. In a 96 well plate, was added at increasing doses (20, 40, 60, 80 and 100µg/mL), and the control was ascorbic acid (Vitamin C). 1mM of DPPH 100µL solution was added to each well, and the samples were incubated in the dark for 30 minutes at room temperature. The solution colour was changed from violet to yellow colour indicate that reactive oxygen species have been scavenged, and it has been measured at 517 nm using the Synergy HT Multimode Reader (Biotek, Winooski, USA). Finally, the percentage of scavenging ability was calculated using the following equation:

$$\% \text{ inhibition} = \frac{Ac - As}{Ac} \times 100$$

Whereas, Ac – OD value of blank, As – OD value of CNPs treated.

Radical scavenging activity by ABTS method

The scavenging activity of CNPs at various concentrations (20 - 100µg/mL) against radicals was evaluated using the ABTS⁺ (2,2'-azinobis(3-ethylbenzothiazoline-6-sulfonic acid) (HiMedia, India) assay, adapting a procedure from a previous study. In the ABTS assay, ascorbic acid was used as the standard antioxidant, and the ability of CNPs to scavenge the ABTS radical (ABTS.ABTS+) was

compared. The ABTS solution was prepared by simply mixing 7mM of aqueous ABTS solution with 2.45mM of potassium persulfate in a dark medium at room temperature for 12 hours. After diluting the same standard solution with ethanol, the ABTS+ reaction mixture was added to each well, and the reaction was measured at 734nm after 10 minutes in the dark using the Synergy HT Multimode Reader (Biotek, Winooski, USA)¹⁵.

RESULT AND DISCUSSION

Analytical characterization of CNPs

UV-Visible spectrophotometer of CNPs

The UV-Vis spectrophotometer investigations have been helpful for structural integrity, changes, and keeping track of the formation of nanoparticles determination¹⁸. The absorption spectra of CNPs were observed at 300nm absorbance, as shown in (Fig.1). The stability of the CNPs was evaluated based on the time intervals from 0 to 60 days as shown in (Fig.2), when the incubation time was increased, a hypochromic shift was observed, which indicates the CNPs are partially stable¹⁹. Strong absorption peaks at 300 nm were visible in the absorption spectra, which is the particular characteristic mentioned in earlier studies²⁰. The interaction of Ce ions with cancer cells and microbes to exhibit anticancer and antibacterial activity, respectively, has been previously reported for CNPs²¹.

SEM Analysis

We examined the topography of the spherical CNPs using a scanning electron

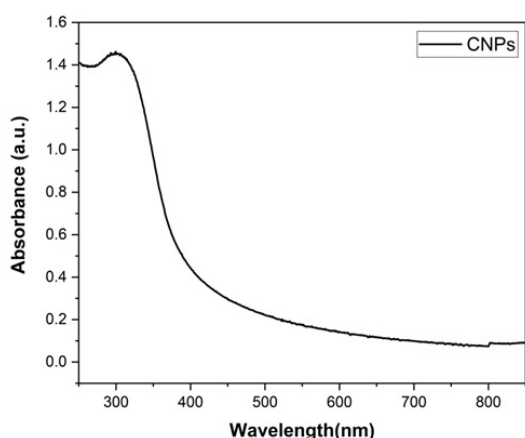


Fig. 1. UV-Vis spectra of CNPs

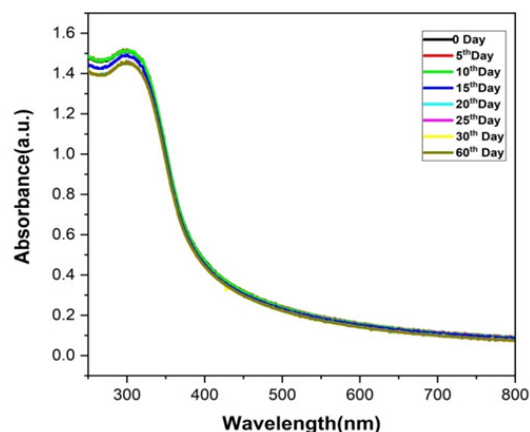


Fig. 2. UV-Vis spectra of CNPs for Stability analyse

microscope, as shown in (Fig.3). The CNPs' spherical appearance and restricted particle range imply that particle distributions are highly constant and that spherical agglomerates have formed. As mentioned in a previous article, synthesis duration, temperature, solvent, and calcination temperature²² are all critical reaction parameters that may explain why this kind of reaction emerges. According to phenomenological evidence, CNPs have a spherical shape with smooth surfaces.

Dynamic light scattering (DLS) analysis was used to investigate the hydrodynamic size distribution of CNPs. The average size of dispersion CNPs was 35 ± 0.4 nm, as shown in (Fig. 4). CNP zeta potential investigation revealed +24.3 mV as shown in (Fig. 5).

Fourier transforms infrared spectroscopy (FT-IR)

The Fourier transform infrared spectroscopy (FT-IR) approach has been shown to be helpful in determining the functional groupings of CNPs, as shown in (Fig.6). This particle absorption at a specific region is observed as minor and major peaks for respective particles. The significant absorption at 3435cm^{-1} in the high-frequency region of the spectrum is due to physically absorbed water, an O-H stretching vibration, or a surface hydroxyl group. The bending vibration of linked structures shows a small shoulder peak at 2073cm^{-1} responsible for (H-O-H). The 1633cm^{-1} peaks are associated with O-C-O symmetric stretching, but the 666 cm^{-1}

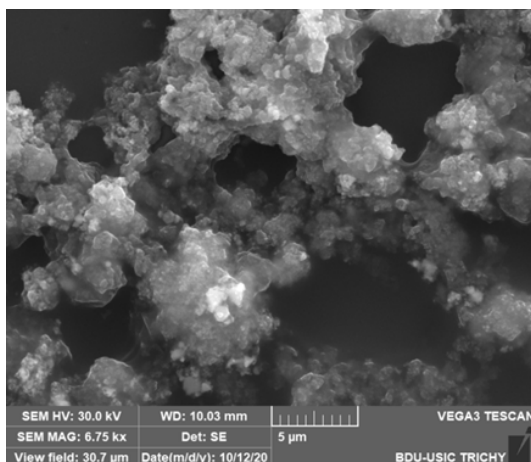


Fig. 3. SEM image of CNPs

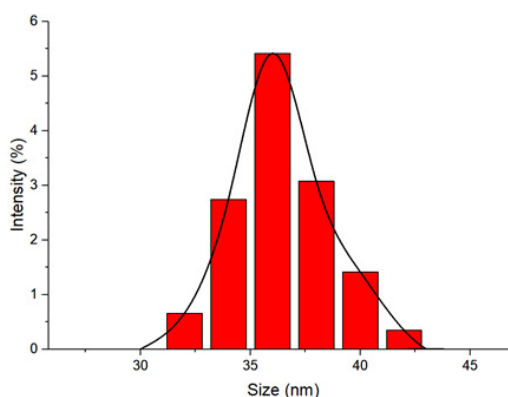


Fig. 4. DLS analysis of CNPs

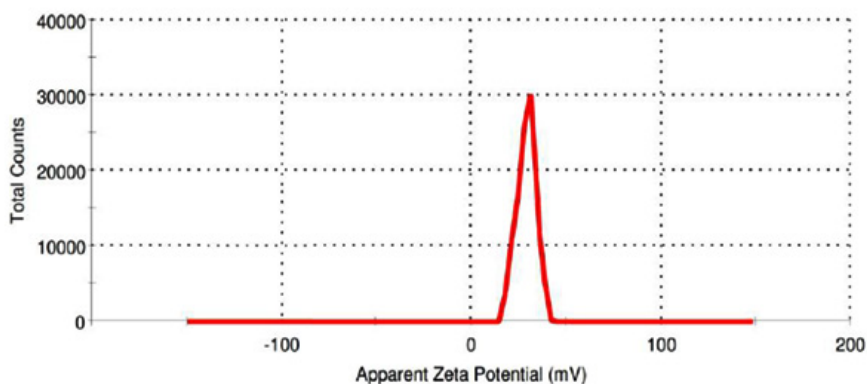


Fig. 5. Zeta potential analysis of CNPs

peaks are directly associated with the frequency of CeO stretching^{8,23}.

XRD analysis of CNPs

CNPs are precipitated, as evidenced by the X-ray diffraction (XRD) pattern in (Fig.7). The XRD pattern of the nanoparticles reveals that they are made of cubic fluorite, CeO₂. For diffraction peaks with values around 28.41°, 32.87°, 47.54°, 56.38°, and 60.18°, the planes (111), (200), (220), (311), and (222) are chosen. This set of peak deflections agrees with the powder X-ray diffraction standard JCPDS No. 34-0394. The XRD pattern showed no peaks related to impurities or other phases, suggesting that the CNPs generated are made of a pure crystal of CeO₂²¹.

Antimicrobial activity Study

CNPs have been tested for antibacterial potential against bacteria such as *S. aureus* and *E.*

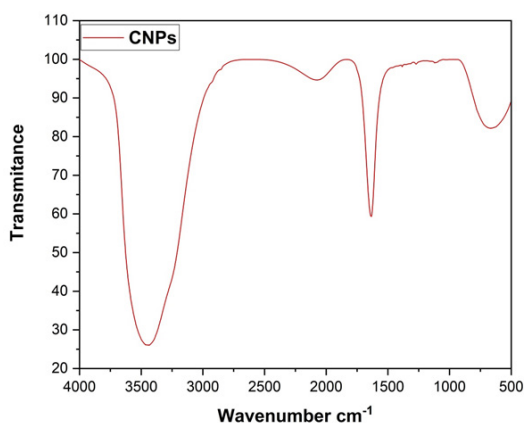


Fig. 6. FT-IR spectra of CNPs

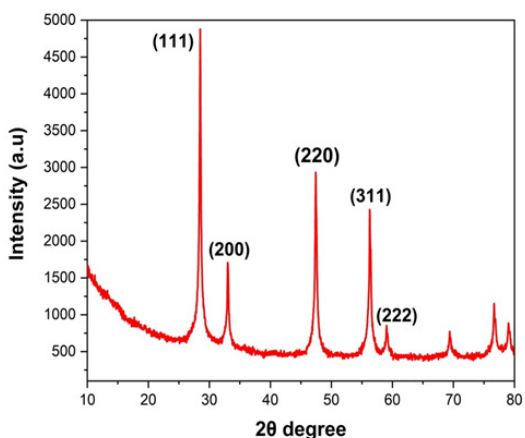


Fig. 7. XRD analyses of CNPs

coli. According to the (Fig. 8) revealed a higher inhibition zone was observed. These findings show that the communication between CNPs and the bacteria's cell wall has efficiently promoted the toxicity of the bacteria and caused cell death. Among the four dosages of CNPs, 100µg/mL depicts a higher inhibition zone for *E. coli* (14 mm) and *S. aureus* (15 mm). The nanoparticles attached to the bacterial cell wall through ionic interactions between negatively charged organisms and positively charged nanoparticles. The binding of CNPs to peptidoglycan consists of gram positive bacteria, which are bound with teichoic acid; this may be a possible interaction with CNPs in antibacterial activity. More importantly, the possible mechanism of antibacterial activity of CNPs may interact with the bacterial cell membrane and bind with the mesosome, which is involved in cellular breathe, ability to cell divide, replicate their DNA, and, ultimately leading to cell death²⁴. The observed antibacterial potential of CNPs at 100 µg/mL concentration exhibits significant efficacy against *S. aureus* and *E. coli*, due to the strong electrostatic forces the nanoparticles attach to the cell membrane to inhibit the growth of bacteria. In an early study, it was reported that CeO₂/GO nanocomposites are potentially active against wound-associated infectious pathogens such as *S. typhi*, *S. aureus*, *E. coli*, and *P. aeruginosa* and present an absence of visible condition²³. The antibacterial activity of Ag-Au loaded CeO₂ nanoparticles against *E. coli* and *S. aureus* has potentially improved compared to other nanocomposite materials due to their

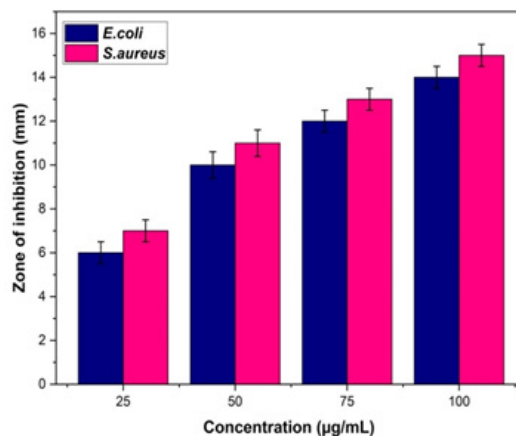


Fig. 8. Antibacterial activity of CNPs against *E. coli* and *S. aureus*

individual metals containing ions²⁵⁻²⁷. The possible mechanism of antibacterial activity has been electrostatic communication between bacterial cell walls and Ag-Au-loaded CeO₂ nanocomposites that influence inhibition of microbial growth and induce microbial death, as reported in past studies^{16, 28-30}. Another mechanism of antibacterial activity reported in previously small nanoparticles has been to easily penetrate inside the cell wall of bacteria and cause cell death^{5,8}. In an early study²¹, CNPs potentially damaged the cell wall of *E. coli* at a concentration of 0.06mg/mL when exposed to X-ray radiation.

Effect of CNPs on bacterial growth

The effect of CNPs on *E. coli* and *S. aureus* growth was demonstrated. The lag, log, stationary, and death phases of *E. coli* and *S. aureus* growth curves were clearly represented in (Fig. 9). While the effect of different doses of CNPs from 25µg/mL to 100µg/mL has been observed, the constriction of the log phase was visible, demonstrating that CNPs have a dose-dependent manner to exploit against *E. coli* and *S. aureus*. The findings could imply that the binding of CNPs to the bacterial cell membrane surface, due to their dual oxidation state of Ce³⁺ and Ce⁴⁺, provided a catalytic site for the bonding and

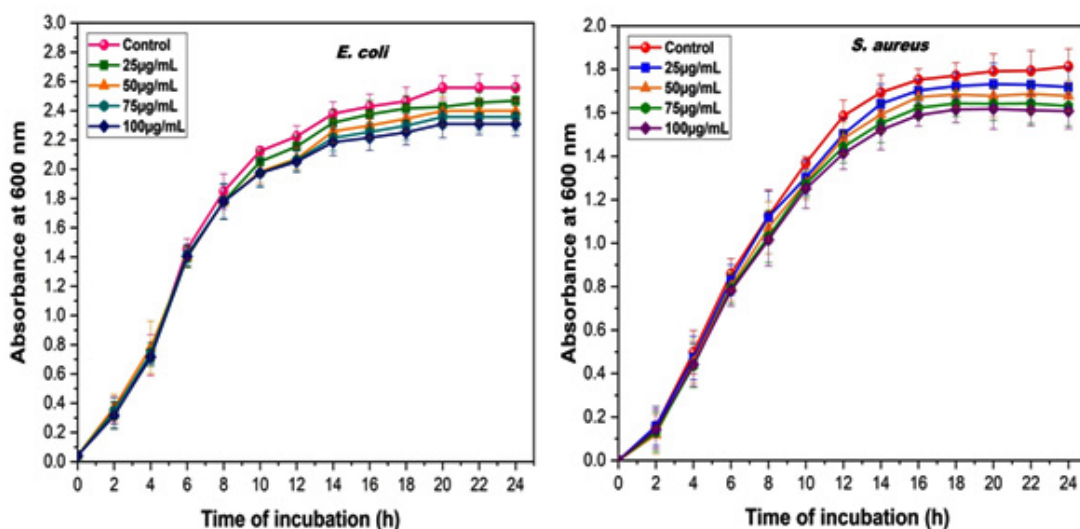


Fig. 9. Growth curve of *E. coli* and *S. aureus* under the CNPs treatment

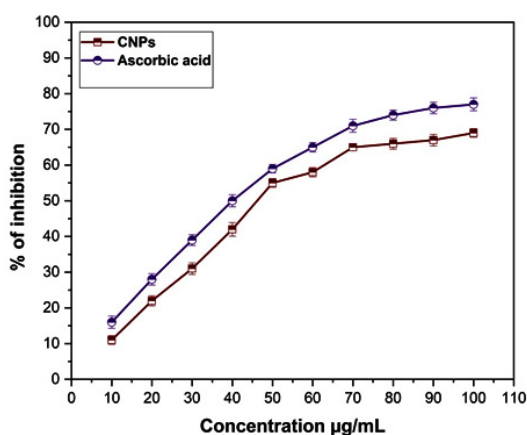


Fig. 10. DPPH radical scavenging activity of CNPs

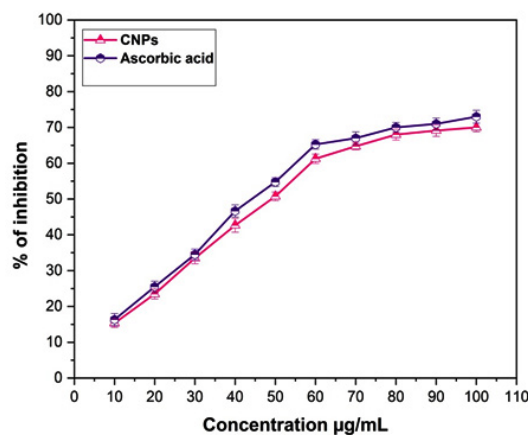


Fig. 11. Antioxidant activity of CNPs using ABTS method

hydrolysis of long-chain phospholipids found on bacteria's cell walls, resulting in cell wall damage and biomass reduction³¹.

Radical Scavenging activity by DPPH method

The antioxidant activity of CNPs was determined using the (DPPH)-2, 2-diphenyl-1-picrylhydrazyl method. When DPPH combines with an antioxidant, it produces a stable free radical that can be converted into a non-radical state. The DPPH radical was initially purple, but an antioxidant converted it to yellow, the colour of the non-radical version. As compared to the industry standard (Vitamin-C), CNPs' free radical scavenging (DPPH) activity revealed significant antioxidant power, with an IC₅₀ percentage of 47.61g/mL as shown in (Fig. 10). A previous study found that the levan coated CNPs have higher antioxidant capacity because polysaccharides contain multiple hydroxyl groups that can react with free radicals, and reduced radical chain reactions are related to antioxidant^{32,33}. The probable mechanism of the radical scavenging potential of cerium oxide nanoparticles, it has a dual oxidation state that converts together based on pH, generating ROS in acidic pH and scavenging the ROS in normal pH, as reported in early study^{34,35}. In DPPH assay 50g/mL of CNPs has highly effective with 87.6% of scavenging potential compared with control α -tocopherol 76.3 % and BHA 52.9% has reported in earlier³⁶. Free radical scavenging activity of nanoceria with a dose dependent manner, which is exposing the concentration of 50 μ g/500 μ l for 48.58% of radical inhibition in an early study, is reported at³². Early studies found that 9mg/mL of CeO₂NPs increased DPPH inhibition by up to 67%, while polysaccharide-coated CeO₂NPs were 85% effective at getting rid of DPPH²¹.

Both solvothermal CeO₂ nanoparticles and hydrothermal CeO₂ nanoparticles were able to get rid of up to 55% and 30% of DPPH, respectively³⁷. The IC50 value for the antioxidant activity of CeO₂ NPs is 4.38 mg/ml. CeO₂ nanoparticles displayed higher antioxidant activity (IC₅₀ = 8-10 mg/mL) than ZnO nanoparticles, according to the literature³⁸⁻⁴⁰. According to past reports, the CNPs have been potentially active against radicals in the concentration range of 0.05g/L upto 0.06g/L when the activity has been low, below the concentration of 0.05g/L⁴¹.

ABTS Radical Scavenging activity

The ABTS method was used to assess the antioxidant activity of CNPs, and the reduction of free radicals caused by the CNPs was seen at 734 nm. CNPs have scavenged free radicals in a dose-dependent manner, with the best scavenging ability being noted in (Fig. 11). The obtained result has depicted that CNPs have a dose-dependent inhibitory effect on the generation of ABTS radicals with an IC₅₀ percentage of 46.26g/mL. It is reasonable to believe that antioxidant capabilities increase directly with nanoparticle concentration¹⁵. ABTS•⁺ scavenging activity of Ce₂O₃NPs is significantly high with 87.2% compared with standard α -tocopherol 74.9 % and BHA 50.1% reported in early study³⁶. In previous report, it was shown that the CNPs have potentially active and scavenged free radicals and inhibit the production of ABTS⁺ radicals in a dose dependent manner compared with Trolox¹⁵. The scavenging potential of *Mentha royleana*-mediated CNPs is 46.7%, compared to 49.7% for control ascorbic acid at an IC₅₀ value of 5.39 g/ml, whereas the IC₅₀ value for *Mentha royleana* was found at a concentration of 5.57g/ml, as reported in an earlier study. The ABTS⁺ radical's species was reduced in proportion to the amount of greenly synthesised CeONPs. Other evidence suggests that CeONPs scavenge ROS from normal cells preferentially, protecting them from reactive oxygen species⁴²⁻⁴⁴.

CONCLUSION

The current study demonstrated cerium oxide nanoparticles (CNPs) have been a considerable help in combating microbial pathogens with significantly formed zones of inhibition against *E.coli* and *S.areus* and reduced biomass with investigation of the bacterial growth curve, which shows considerably reduced growth of *E.coli* and *S.areus* in a dose dependent manner up to the incubation period of 24 hours. The ionic interaction between CNPs and bacterial cell membranes is crucial to their antibacterial activity. This is because the CNPs dual oxidation state of Ce³⁺ and Ce⁴⁺ surface provides a catalytic site for the attachment and hydrolysis of long-chain phospholipids found on the cell wall of bacteria, damaging the cell wall and decreasing

the biomass. The obtained results from the present study unequivocally proved CNPs have good antibacterial properties. DPPH and ABTS are the methods that were used to investigate the *in vitro* antioxidant activity of CNPs. In the DPPH assay, the CNPs have an IC₅₀ concentration of 47.61 µg/mL, which yields a significant result when compared with the control. The result that was obtained from this study, which was the ABTS radical scavenging assay of CNPs, demonstrated that there was an inhibition of ABTS radical production in a dose-dependent manner, in addition to a significant IC₅₀ concentration of 46.26 µg/mL. This finding was made possible by the fact that the ABTS radical scavenging assay of CNPs was conducted. According to the results that were obtained, CNPs have beneficial antioxidant properties, with the paired oxidation states Ce³⁺ and Ce⁴⁺ that contain CNPs having the most significant influence. The SEM, XRD, DLS, Zeta potential, FTIR and UV-Visible spectrophotometer characterizations studies are supported to the antibacterial and antioxidant activity properties of CNPs. Thus, the present study demonstrated that cerium oxide nanoparticles could be used as effective antimicrobial and antioxidant agents. In our subsequent research, we focused on the toxicity of CNPs that had been functionalized with phytochemicals in both *in vitro* and *in vivo* studies to better understand the potential mechanisms involved.

ACKNOWLEDGMENTS

The authors are grateful to Bharathidasan University for having received Department of Science and Technology Science and Engineering Research Board Empowerment and Equity (DST-SERB-EEQ), Government of India, project fellow Ref. No. 03056/P4/2019 Dated 28.06.2019.

Conflict of Interest

The authors declare no conflict of interest.

Funding Sources

This work was supported by Department of Science and Technology Science and Engineering Research Board Empowerment and Equity (DST-SERB-EEQ), Government of India, Ref. No. 03056/P4/2019 Dated 28.06.2019. Dr. K. Premkumar has received research support from Bharathidasan University, Trichy.

REFERENCES

1. Nithya P, Sundrarajan M Ionic liquid functionalized biogenic synthesis of AgAu bimetal doped CeO₂ nanoparticles from *Justicia adhatoda* for pharmaceutical applications: Antibacterial and anti-cancer activities. *Journal of Photochemistry and Photobiology B: Biology*. 2020; 202:111706. <https://doi.org/10.1016/j.jphotobiol.2019.111706>
2. Liang Y, Guo N, Li L, Ji G, Gan S Fabrication of porous 3D flower-like Ag/ZnO heterostructure composites with enhanced photocatalytic performance. *Applied Surface Science*. 2015;332:32-9. <https://doi.org/10.1016/j.apsusc.2015.01.116>
3. Farokhzad OC, Langer R Impact of nanotechnology on drug delivery. *ACS nano*. 2009;3(1):16-20. <https://doi.org/10.1021/nn900002m>
4. Ghibelli L, Mathur S. Biological interactions of oxide nanoparticles: The good and the evil. *Mrs Bulletin*. 2014;39(11):949-54. DOI: <https://doi.org/10.1557/mrs.2014.250>
5. Magdalane CM, Kaviyarasu K, Raja A, Arularasu MV, Mola GT, Isaev AB, Al-Dhabi NA, Arasu MV, Jeyaraj B, Kennedy J, Maaza M. Photocatalytic decomposition effect of erbium doped cerium oxide nanostructures driven by visible light irradiation: investigation of cytotoxicity, antibacterial growth inhibition using catalyst. *Journal of Photochemistry and Photobiology B: Biology*. 2018;185:275-82. <https://doi.org/10.1016/j.jphotobiol.2018.06.011>
6. Magdalane CM, Kaviyarasu K, Vijaya JJ, Siddhardha B, Jeyaraj B Facile synthesis of heterostructured cerium oxide/yttrium oxide nanocomposite in UV light induced photocatalytic degradation and catalytic reduction: synergistic effect of antimicrobial studies. *Journal of Photochemistry and Photobiology B: Biology*. 2017; 173:23-34. <https://doi.org/10.1016/j.jphotobiol.2017.05.024>
7. Dhall A, Self W Cerium oxide nanoparticles: a brief review of their synthesis methods and biomedical applications. *Antioxidants*. 2018;7(8):97. <https://doi.org/10.3390/antiox7080097>
8. Khadar YS, Balamurugan A, Devarajan VP, Subramanian R, Kumar SD. Synthesis, characterization and antibacterial activity of cobalt doped cerium oxide (CeO₂: Co) nanoparticles by using hydrothermal method. *Journal of Materials Research and Technology*.

- 2019;8(1):267-74. <https://doi.org/10.1016/j.jmrt.2017.12.005>
9. Masui T, Fujiwara K, Machida KI, Adachi GY, Sakata T, Mori H. Characterization of cerium (IV) oxide ultrafine particles prepared using reversed micelles. *Chemistry of Materials*. 1997;9(10):2197-204. <https://doi.org/10.1021/cm970359v>
 10. Abbas F, Jan T, Iqbal J, Ahmad I, Naqvi MS, Malik M. Facile synthesis of ferromagnetic Ni doped CeO₂ nanoparticles with enhanced anticancer activity. *Applied Surface Science*. 2015;357:931-6. <https://doi.org/10.1016/j.apsusc.2015.08.229>
 11. Azad AM, Matthews T, Swary J. Processing and characterization of electrospun Y₂O₃-stabilized ZrO₂ (YSZ) and Gd₂O₃-doped CeO₂ (GDC) nanofibers. *Materials Science and Engineering: B*. 2005;123(3):252-8. <https://doi.org/10.1016/j.mseb.2005.08.070>
 12. Khulbe K, Karmakar K, Ghosh S, Chandra K, Chakravorty D, Muges G. Nanoceria-based phospholipase-mimetic cell membrane disruptive antibiofilm agents. *ACS Applied Bio Materials*. 2020; 3(7):4316-28. <https://doi.org/10.1021/acsbm.0c00363>
 13. Pinna A, Figus C, Lasio B, Piccinini M, Malfatti L, Innocenzi P. Release of ceria nanoparticles grafted on hybrid organic-inorganic films for biomedical application. *ACS Applied Materials & Interfaces*. 2012;4(8):3916-22. <https://doi.org/10.1021/am300732v>
 14. Pinna A, Cali E, Kerherve G, Galleri G, Maggini M, Innocenzi P, Malfatti L. Fulleropyrrolidine-functionalized ceria nanoparticles as a tethered dual nanosystem with improved antioxidant properties. *Nanoscale Advances*. 2020;2(6):2387-96. DOI: 10.1039/D0NA00048E
 15. Pop OL, Mesaros A, Vodnar DC, Suharoschi R, Tăbăran F, Mageru'an L, Tóдор IS, Diaconeasa Z, Balint A, Ciontea L, Socaciu C. Cerium oxide nanoparticles and their efficient antibacterial application in vitro against gram-positive and gram-negative pathogens. *Nanomaterials*. 2020;10(8):1614. <https://doi.org/10.3390/nano10081614>
 16. Deepika MS, Thangam R, Vijayakumar TS, Sasirekha R, Vimala RT, Sivasubramanian S, Arun S, Babu MD, Thirumurugan R. Antibacterial synergy between rutin and florfenicol enhances therapeutic spectrum against drug resistant *Aeromonas hydrophila*. *Microbial pathogenesis*. 2019;135:103612. <https://doi.org/10.1016/j.micpath.2019.103612>
 17. Brand-Williams W, Cuvelier ME, Berset CL. Use of a free radical method to evaluate antioxidant activity. *LWT - Food Sci Technol*. 1995; 28(1), 25-30. [https://doi.org/10.1016/S0023-6438\(95\)80008-5](https://doi.org/10.1016/S0023-6438(95)80008-5)
 18. Deepika MS, Thangam R, Sheena TS, Sasirekha R, Sivasubramanian S, Babu MD, Jeganathan K, Thirumurugan R. A novel rutin-fucoidan complex based phytotherapy for cervical cancer through achieving enhanced bioavailability and cancer cell apoptosis. *Biomedicine & Pharmacotherapy*. 2019 ;109:1181-95. <https://doi.org/10.1016/j.biopha.2018.10.178>
 19. Badi'ah HI, Seede F, Supriyanto G, Zaidan AH. Synthesis of silver nanoparticles and the development in analysis method. In *IOP Conf. Ser.: Earth Environ. Sci.*, 2019; (Vol. 217, No. 1, p. 012005). IOP Publishing. <https://doi.org/10.1088/1755-1315/217/1/012005>
 20. Parimi D, Sundararajan V, Sadak O, Gunasekaran S, Mohideen SS, Sundaramurthy A (2019) Synthesis of positively and negatively charged CeO₂ nanoparticles: investigation of the role of surface charge on growth and development of *Drosophila melanogaster*. *ACS omega*. 4(1):104-13. <https://doi.org/10.1021/acsomega.8b02747>
 21. Nurhasanah I, Safitri W, Arifin Z, Subagio A, Windarti T. Antioxidant activity and dose enhancement factor of CeO₂ nanoparticles synthesized by precipitation method. In *IOP Conference Series: Materials Science and Engineering 2018*; (Vol. 432, No. 1, p. 012031). IOP Publishing. <https://doi.org/doi:10.1088/1757-899X/432/1/012031>
 22. Habib IY, Kumara NT, Lim CM, Mahadi AH. Dynamic light scattering and zeta potential studies of ceria nanoparticles. In *Solid State Phenomena*. 2018; (Vol. 278, pp. 112-120). Trans Tech Publications Ltd. <https://doi.org/10.4028/www.scientific.net/SSP.278.112>
 23. Sharma G, Prema D, Venkataprasanna KS, Prakash J, Sahabuddin S, Venkatasubbu GD. Photo induced antibacterial activity of CeO₂/GO against wound pathogens. *Arabian Journal of Chemistry*. 2020;13(11):7680-94. <https://doi.org/10.1016/j.arabjc.2020.09.004>
 24. Gopinath K, Karthika V, Sundaravadivelan C, Gowri S, Arumugam A. Mycogenesis of cerium oxide nanoparticles using *Aspergillus niger* culture filtrate and their applications for antibacterial and larvicidal activities. *Journal of Nanostructure in Chemistry*. 2015; 5(3):295-303. <https://doi.org/10.1007/s40097-015-0161-2>
 25. Xia T, Kovochich M, Brant J, Hotze M, Sempf

- J, Oberley T, Sioutas C, Yeh JI, Wiesner MR, Nel AE. Comparison of the abilities of ambient and manufactured nanoparticles to induce cellular toxicity according to an oxidative stress paradigm. *Nano letters*. 2006;6(8):1794-807. <https://doi.org/10.1021/nl061025k>
26. Xia T, Kovochich M, Liang M, Madler L, Gilbert B, Shi H, Yeh JI, Zink JI, Nel AE. Comparison of the mechanism of toxicity of zinc oxide and cerium oxide nanoparticles based on dissolution and oxidative stress properties. *ACS nano*. 2008;2(10):2121-34. <https://doi.org/10.1021/nl080511k>
27. Burello E, Worth AP. A theoretical framework for predicting the oxidative stress potential of oxide nanoparticles. *Nanotoxicology*. 2011;5(2):228-35. <https://doi.org/10.3109/17435390.2010.502980>
28. Agarwal H, Menon S, Kumar SV, Rajeshkumar S. Mechanistic study on antibacterial action of zinc oxide nanoparticles synthesized using green route. *Chemico-biological interactions*. 2018;286:60-70. <https://doi.org/10.1016/j.cbi.2018.03.008>
29. Cedervall T, Lynch I, Lindman S, Berggård T, Thulin E, Nilsson H, Dawson KA, Linse S. Understanding the nanoparticle-protein corona using methods to quantify exchange rates and affinities of proteins for nanoparticles. *Proceedings of the National Academy of Sciences*. 2007;104(7):2050-5. <https://doi.org/10.1073/pnas.0608582104>
30. Azzam EM, Zaki MF. Surface and antibacterial activity of synthesized nonionic surfactant assembled on metal nanoparticles. *Egyptian Journal of Petroleum*. 2016;25(2):153-9. <https://doi.org/10.1016/j.ejpe.2015.04.005>
31. Chatterjee S, Bandyopadhyay A, Sarkar K. Effect of iron oxide and gold nanoparticles on bacterial growth leading towards biological application. *Journal of Nanobiotechnology*. 2011;9(1):1-7. doi:10.1186/1477-3155-9-34
32. Pitchumani Krishnaveni M, Annadurai G. Biosynthesis of nanoceria from bacillus subtilis: characterization and antioxidant potential. *Res J Life Sci*. 2019;5(3):644. <https://doi.org/10.26479/2019.0503.52>
33. Pozharitskaya ON, Obluchinskaya ED, Shikov AN. Mechanisms of bioactivities of fucoidan from the brown seaweed *Fucus vesiculosus* L. of the Barents Sea. *Marine drugs*. 2020; 18(5):275. <https://doi.org/10.3390/md18050275>
34. Asati A, Santra S, Kaittanis C, Perez JM. Surface-charge-dependent cell localization and cytotoxicity of cerium oxide nanoparticles. *ACS nano*. 2010;4(9):5321. <https://doi.org/10.1021/nn100816s>
35. Nourmohammadi E, Khoshdel-Sarkarizi H, Nedaeinia R, Sadeghnia HR, Hasanzadeh L, Darroudi M, Kazemi oskuee R. Evaluation of anticancer effects of cerium oxide nanoparticles on mouse fibrosarcoma cell line. *Journal of cellular physiology*. 2019;234(4):4987-96. <https://doi.org/10.1002/jcp.27303>
36. Nadaroglu H, Onem H, Alayli Gungor A. Green synthesis of Ce2O3 NPs and determination of its antioxidant activity. *IET nanobiotechnology*. 2017;11(4):411-9. <https://doi.org/10.1049/iet-nbt.2016.0138>
37. Soren S, Jena SR, Samanta L, Parhi P. Antioxidant potential and toxicity study of the cerium oxide nanoparticles synthesized by microwave-mediated synthesis. *Applied biochemistry and biotechnology*. 2015;177:148-61. DOI 10.1007/s12010-015-1734-8
38. Nethravathi PC, Shruthi GS, Suresh D, Nagabhushana H, Sharma SC. Garcinia xanthochymus mediated green synthesis of ZnO nanoparticles: photoluminescence, photocatalytic and antioxidant activity studies. *Ceramics International*. 2015;41(7):8680-7. <https://doi.org/10.1016/j.ceramint.2015.03.084>
39. Suresh D, Shobharani RM, Nethravathi PC, Kumar MP, Nagabhushana H, Sharma SC. Artocarpus gomezianus aided green synthesis of ZnO nanoparticles: Luminescence, photocatalytic and antioxidant properties. *Spectrochimica Acta Part A: Molecular and Biomolecular Spectroscopy*. 2015;141:128-34. <https://doi.org/10.1016/j.saa.2015.01.048>
40. Madan HR, Sharma SC, Suresh D, Vidya YS, Nagabhushana H, Rajanaik H, Anantharaju KS, Prashantha SC, Maiya PS. Facile green fabrication of nanostructure ZnO plates, bullets, flower, prismatic tip, closed pine cone: their antibacterial, antioxidant, photoluminescent and photocatalytic properties. *Spectrochimica Acta Part A: Molecular and Biomolecular Spectroscopy*. 2016;152:404-16. <https://doi.org/10.1016/j.saa.2015.07.067>
41. Al-Mashhadani AH. Study of in vitro and in vivo free radical scavenging activity for radioprotection of cerium oxide nanoparticles. *Iraqi Journal of Physics*. 2017;15(35):40-7. <https://doi.org/10.30723/ijp.v15i35.52>
42. Aseyd Nezhad S, Es hagh A, Tabrizi MH. Green synthesis of cerium oxide nanoparticle using *Origanum majorana* L. leaf extract,

- its characterization and biological activities. *Applied Organometallic Chemistry*. 2020 Feb;34(2):e5314. <https://doi.org/10.1002/aoc.5314>.
43. Homayouni-Tabrizi M, Asoodeh A, Mashreghi M, Rezazade Bazaz M, Kazemi Oskuee R, Darroudi M. Attachment of a frog skin-derived peptide to functionalized cerium oxide nanoparticles. *International Journal of Peptide Research and Therapeutics*. 2016 Dec;22:505-10. <https://doi.org/10.1007/s10989-016-9531-y>.
44. Khan M, Raja NI, Asad MJ, Mashwani ZU. Antioxidant and hypoglycemic potential of phytogetic cerium oxide nanoparticles. *Scientific Reports*. 2023 Mar 18;13(1):4514. <https://doi.org/10.1038/s41598-023-31498-8>.